Photo-controllable Dynamic Chemistry of Intercalated Organic Disulfides: A Strategy for Flexible Functionalization

Jonathon Tanks,*[1] Takashi Hiroi,[2] Kenji Tamura,[3] and Kimiyoshi Naito[1,4]

[1]Research Center for Structural Materials, National Institute for Materials Science (NIMS), 1-2-1 Sengen, Tsukuba, Ibaraki 305-0047

[2]International Center for Young Scientists, National Institute for Materials Science (NIMS), 1-2-1 Sengen, Tsukuba, Ibaraki 305-0047

[3]Research Center for Functional Materials, National Institute for Materials Science (NIMS), 1-1 Namiki, Tsukuba, Ibaraki 305-0044

[4]Department of Aerospace Engineering, Tohoku University, 6-6-1 Aramaki-aza-aoba, Sendai, Miyagi 980-8579

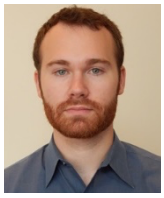

E-mail: tanks.jonathon@nims.go.jp

Jonathon Tanks
Jonathon Tanks is a Research Scientist at the National Institute for Materials Science (NIMS). He received his Ph.D. in Chemical Science and Engineering from the Tokyo Institute of Technology in 2019 under the supervision of Prof. Masatoshi Kubouchi.

Abstract

The dynamic covalent chemistry of molecular disulfides has been studied extensively in solution, but their reactivity when confined to nanospaces has not been investigated, nor has their application to functional nanomaterials been explored. In this study, symmetrical organic disulfides were tethered to the basal planes of synthetic mica by intercalation, confining photo-induced reactions to the interlayer as a result. This approach functionalizes the nanosheets to act as host for photo-induced disulfide-disulfide, disulfide-thiol, and disulfide-ene reactions, providing control and versatility for a wide variety of applications.

Keywords: Disulfide chemistry, Layered silicates, Photo-reactivity

1. Introduction

Functionalized inorganic nanosheets represent a key demographic in the world of materials science, including natural and synthetic silicates and layered double hydroxides. While exfoliation into few-layer nanosheets is important for catalysts and polymer nanocomposites, intercalation provides certain structures and functions for catalytic, contaminant removal, and biomedical applications.[1,2] In particular, thiol functionalization is extremely versatile and can provide the ability to bond with metals, conjugated carbons (alkenes, alkynes), acid halides, epoxide, and other thiols.[3] However, while their high reactivity toward metals can lead to unwanted reactions and thus requires protection/deprotection in some reaction systems, a catalyst is often needed for anionic- or radical-type ligand/polymer reactions, complicating the synthesis procedure depending on the functional groups and substrates involved.[4,5]

One strategy to control the reactivity of thiols is to start from the oxidized form, disulfide, and use reduction or radical attack to generate the reactive sulfur atoms.[5,6] Furthermore, disulfides exhibit unique dynamic bonding behavior, exchanging with other disulfides and thiols through metathesis or redox pathways, the former of which may be anion- or radical-mediated.[6-11] Even without chemical catalysts (e.g., nucleophile, radical initiator) or stimulus (e.g., light, heat), these exchange reactions can reach equilibrium in hours or days, depending on the solvent.[7,9] We describe these as so-called "indiscriminate" reactions, due to lack of spatial or temporal control.

It has been demonstrated that adding a nucleophilic catalyst or radical initiator accelerates reaction rates between aryl disulfides in DMSO by roughly 4-5 times or 2-3 times, respectively, through their corresponding pathways.[7] By contrast, because disulfides readily form thiyl radicals by UV radiation, photo-induced exchange reactions can occur at room temperature without chemical catalysts at rates nearly 30 times higher.[7-9] For a given set of conditions, the reaction can only be accelerated but not slowed or delayed, aside from adding radical scavengers—which may have undesirable side effects.

Recombination after photolysis occurs if the generated radical species are in close proximity and not immediately solvated, whereas solvated polar radicals survive long enough to attack other disulfide bonds and propagate the exchange reaction.[11] Thus, system factors such as solvent, concentration, and stimuli or catalysts—not to mention reagent characteristics like disulfide molecular structure—greatly affect how the reaction proceeds.

Interestingly, experimental and computational studies revealed that the half-life of thiyl radicals covalently bound to nanoporous silica was prolonged to 65 h, compared to just 200 μs in solution.[12] These findings suggest that anchoring disulfides to a substrate may be a simple strategy for reducing so-called "indiscriminate" reactions through conformational constraint and physical proximity. In this study, we aimed to functionalize nanosheets with disulfides to create a versatile material with unique functionality, and subsequently demonstrated that interlayer confinement helps control reactivity and stability without significant changes in photo-induced reaction rates.

To date, inserting disulfides into layered materials has only been reported for facilitating the exfoliation of MOFs to increase their catalytic efficiency,[13] but the scope was limited to treating the disulfide as a chemically labile bond to break via reduction. The structure and reactivity of disulfide-

functionalized layered materials has not been explored. This new family of materials represents a reactive substrate which can be used for catalysis, in-situ polymerization, protein/DNA modification, contaminant capture, and nanoarchitecture applications via a wide variety of redox, anion, and radical pathways (Fig. 1a).

Herein, we functionalized the interlayer space of a cation-type synthetic mica (Na-TSM, cation exchange capacity (CEC) ≈ 1.2 meq/g) with two organic disulfides, 4-aminophenyldisulfide (APDS) and cystamine (Cyst), using an intercalation approach (Fig. 1a). Our report is organized as follows: the intercalation structure is briefly described, followed by a demonstration of photo-induced disulfide exchange reactions in the interlayer, and concluded with a demonstration of disulfide-initiated in-situ alkene polymerization in the interlayer.

2. Results and Discussion

We first characterized the reagent powders APDS and Cyst, and the intercalated silicates APDS-TSM and Cyst-TSM; see the ESI for more detailed description. In brief, XRD and Raman analyses revealed that the APDS conformation changes from *gauche* in the reagent powder to *anti* in the interlayer, while Cyst remains a seemingly random mixture of multiple conformers before and after intercalation (Fig. S2 and S3, ESI). The conformation affects both the basal spacing and the reactivity.[12] Aromatic APDS is more rigid than aliphatic Cyst and is thus better able to pack into the interlayer, significantly increasing the basal spacing d_{001} (Fig. 1b). This resulted in disulfide contents of 0.69 mmol/g and 0.58 mmol/g for APDS-TSM and Cyst-TSM, respectively, in terms of TSM weight (Fig. S4, ESI). The proposed intercalation structures are illustrated in Fig. 1c, and the stacking morphology is shown in Fig. S5 (ESI).

All reaction experiments were conducted in DMSO, a common solvent in disulfide chemistry.[6,7,15] DMSO showed a remarkable swelling effect on the disulfide-functionalized silicates, as seen by the very weak d_{001} and d_{002} reflections and the lack of other characteristic basal diffraction peaks (Fig. S6, ESI). The especially large d_{001} value of APDS-TSM (26.5 Å) means that the interlayer spacing is roughly equivalent to or greater than the length of a vertically oriented *anti*-APDS molecule (Fig. S3, ESI). This indicates an extensive degree of delamination,[1,14] which was supported by Tyndall light scattering and AFM measurements of APDS-TSM (Fig. S6, ESI) that seem to show a trend of fewer layers in DMSO than water. Furthermore, the original XRD patterns and UV-vis spectra were obtained from silicates that were recovered from DMSO by solvent evaporation, confirming that the changes in the intercalation structure by solvent swelling are reversible (Fig. S6, ESI).

We next demonstrate the UV-controllable dynamic bonding nature of the functional nanosheets—the initial objective of our research. Photo-induced exchange reactions (PER) were conducted between 4-nitrophenyl disulfide (NPDS)—selected as a spectroscopically detectable reactant—and APDS (**PER1**), $APDS_{10}$-TSM (**PER2**), or Cyst-TSM (**PER3**). Fig. 2a-c shows the time-resolved UV-vis spectra and peak absorbances of **PER1** and **PER2** for comparison; see the ESI for **PER3** (Fig. S7, ESI). The production of asymmetrical disulfides could be observed by monitoring the consumption of NPDS at 322 nm. Note that the initial reaction rates for molecular APDS in solution and in the TSM interlayer are nearly identical (Fig. 2d). A small peak at 496 nm, corresponding to both thiolate anions and thiyl radicals, suddenly appeared upon irradiation and reached a maximum around their respective half-lives, then decayed to nearly zero as the reaction reached equilibrium. These results, along with a lack of distinct isosbestic points, suggest a multistep process rather than simple conversion to a single product, which is corroborated by previous reports.[7,10,15]

Encouraged by the prospect that intercalation does not alter the disulfide's photo-reactivity, we wished to observe the so-called indiscriminate disulfide exchange in DMSO without UV radiation. However, while the reaction between molecular APDS and NPDS did indeed proceed at room temperature in the dark (Fig. S8a, ESI), nothing happened with APDS-TSM. Intrigued by this unexpected result, we repeated the conditions of **PER1** and **PER2** but stopped after 20 min of irradiation and measured the UV-vis spectra after 24 h. Molecular APDS and NPDS continue to undergo metathesis after radiation, but APDS-TSM showed no significant change in either peak of interest, further pointing to the presence of stable intermediate species. XRD measurements of the **PER2** silicates collected after the reaction show an increase in d_{001} of roughly 8 Å, confirming scission of the original APDS disulfide linkages between TSM layers (Fig. S6c, ESI).

Cyst-TSM was generally similar but a minute progression of the reaction could be perceived (Fig. S7c). We speculate this difference is because aliphatic Cyst has numerous conformers that allow thiyl radicals to react easily, whereas aromatic APDS does not react with its neighbors as it would form the energetically unstable *syn* conformer.[12]

We propose that tethering organic disulfides to the basal planes of TSM physically hinders them from freely reacting without UV radiation and simultaneously prolongs the thiyl radical lifetime, thus imparting controllable reactivity via the silicate substrate.[12] Furthermore, the conditions of **PER2** was repeated using the APDS-TSM recovered from DMSO (mentioned above) and we found no significant change compared to the original unswollen APDS-TSM material (Fig. S8b). This indicates that the disulfide-intercalated nanosheets retain their functionality and can be reused even after delamination in strong polar solvent.

Disulfide-thiol exchange reactions were not investigated in depth in the current work, but β-mercaptoethanol (β-ME) and 1-decanethiol (1-DT) were used in a cursory study to observe the PER (see the ESI).

Next, let us shift our perspective from the effect of interlayer tethering on disulfide chemistry, to the functionality of the nanosheets. In-situ polymerization involving nanosheets can be challenging using conventional free radical polymerization approaches, since typical radical initiators (AIBN, TPO, etc.) indiscriminately react with the monomers without sufficiently penetrating the interlayer. Several attempts have been made to synthesize linear polymers by tethering a stable radical or trithiocarbonate RAFT agent to the silicates,[16] but the need for separate initiators or synthesis of novel intercalating agents is disadvantageous and their versatility as a functionalized nanomaterial is limited.

We further demonstrated the UV-controllable reactivity of the layered silicates by in-situ polymerization of an acrylic monomer (pentaerythritol triacrylate, PETA) using only the intercalated disulfides as dual photoinitiator/chain transfer agent. The resulting films are not intended for a specific application, but only serve to demonstrate thiyl radical-initiated polymerization that starts from the interlayer. Future work will apply this technology to various polymerization systems as a strategy to fabricate advanced functional composite materials.

A total of six formulations were compared, where films were fabricated by UV radiation and monitored by ATR-FTIR: three control films containing no disulfide and three proof-of-

concept films containing disulfides (see ESI for more details). Fig. 4a shows the relative curing rates as they relate to radical generation and propagation. The PETA film containing only APDS-TSM (no photoinitiator) cured at a rate comparable to the PETA film containing photoinitiator TPO with Na-TSM (no disulfide), indicating that disulfides tethered to the interlayer do indeed initiate radical polymerization. We confirmed that the thiyl radicals are responsible for polymerization rather than the silicate itself by adding unreactive Na-TSM to the PETA monomer without TPO and no curing was detectable within 20 min of radiation (see ESI). Although molecular disulfides have been used as photoinitiators for polymerization in solution,[7,10] this is the first report (to our knowledge) of in-situ polymerization initiated by disulfides anchored to the basal planes of layered materials.

Not only do intercalated disulfides initiate polymerization, they also improve exfoliation in the nanocomposite. XRD patterns of the films (Fig. 4b) show the original d_{001} peak (see Fig. 1b) in the case of Na-TSM, whereas APDS-TSM shows a drastically reduced peak. The broad rise below 2.5° for APDS-TSM strongly suggests delamination, which is not present for Na-TSM. Furthermore, the Na-TSM film is cloudy while the APDS-TSM is highly transparent (Fig. 4b). Thus, we propose that tethering APDS to the interlayer facilitates exfoliation simply by ensuring the photo-induced polymerization starts from the interlayer and propagates outward.

The Raman spectrum of the APDS-TSM film (Fig. 4c) shows the C-S peaks (660 cm^{-1}) but no S-S peaks were detectable, whereas neither peak was observed for the Na-TSM film. This supports our assertion that UV radiation generates thiyl radicals in the interlayer which then react with the alkene monomer. Cyst-TSM also shows a C-S peak but no S-S peak, as well as signs of partial exfoliation (Fig. S10). This suggests that Cyst-TSM produces thiyl radicals for in-situ polymerization like APDS-TSM, but a smaller initial d_{001} limits monomer penetration in the interlayer and results in a lower degree of exfoliation. Substituting APDS with 4,4′-aminophenyl sulfide (APS) in the interlayer of TSM resulted in no film formation compared to APDS-TSM or Cyst-TSM. Thus, we conclude that S-S scission is the source of radical generation, not C-S scission (Fig. S10).

3. Conclusion

In summary, we have synthesized novel disulfide-functionalized layered silicates and demonstrated their reactivity through photo-induced disulfide exchange reactions in solution and in-situ polymerization via disulfide-ene reactions. Whereas free disulfides undergo indiscriminate metathesis in certain solvents, tethering them to the basal planes of layered materials controls their photo-reactivity through physical constraint. The versatility of these 2D substrates is anticipated to lead to numerous applications including photocatalysts, nanocomposites, and even biological materials.

4. Experimental

Materials. Na^+-type fluorotetrasilicic mica, Na-TSM with the chemical formula $Na_{0.85}[(Mg_{2.10}Al_{0.01}Li_{0.02})Si_4O_{10}](F_{1.47} \cdot (OH)_{0.53})$ (CEC ≈ 1.2 meq/g; analysis by Ca adsorption method, Topy Industries, Ltd)[S1] was provided by Topy Industries, Ltd. 4-Aminophenyldisulfide (APDS), and cystamine dihydrochloride (Cyst) were purchased from Sigma Aldrich, and 4-nitrophenyl disulfide (NPDS), β-mercaptoethanol (BME), and Trimethylbenzoyldiphenyl phosphine oxide (TPO) were purchased from Tokyo Chemical Industry, Ltd. (TCI). All reagents were used as received. Pentaerythritol triacrylate (PETA) was purchased from Toagosei Co., Ltd, and DMSO was used as received from Nacalai Tesque, Inc.

Preparation of Disulfide-intercalated Silicates. APDS (248.37 g/mol) was first protonated with HCl (2.0 eq.) in ultra-pure water at 40 °C, then cooled to room temperature to yield a 20 mM solution. Cyst (225.19 g/mol), which was received in its protonated form, was also dissolved in ultra-pure water at a concentration of 20 mM. APDS-TSM and Cyst-TSM were prepared by mixing Na-TSM (2 g) into ultra-pure water by magnetic stirrer for at least 2 h, then the appropriate amount of disulfide solution was added and the dispersion was further stirred for at least 24 h. The initial watervolume was adjusted so that total water volume (after addition of the disulfide solution) was held constant at 200 mL. The amount of added disulfide was set at 10xCEC, which corresponds to 60 mmol/L, since the disulfides in our study are diamine-type. The intercalated crystals were collected via centrifugation (15k rpm, 10 min) and washed with water/ethanol (50/50 vol.) at least three times, then dried in a circulating oven at 40 °C.

Disulfide Exchange Reactions. UV-vis calibration curves were obtained for the reagents and silicates by preparing solutions and dispersions as described above (Fig. S1a,b). The conditions and procedure for the photo-induced exchange reaction (PER) are as follows: 3 mL of solution was irradiated in a quartz cuvette using a high-pressure mercury lamp (SX-UI251HQ, Ushio Inc.; 1.7 mW/cm^2 @ 300 nm) at a distance of 50 mm, and UV-vis spectra were taken at 5- or 10-min intervals. Disulfide exchange was monitored by calculating the remaining molar concentration of NPDS as $C_{NPDS} = C_0 - (\Delta A_{322})/m$, where m is the slope of the calibration curve. The reactant concentrations were adjusted to optimize the broad peak between 300-330 nm, such that the equimolar reaction of molecular disulfides (**PER1**) involved 0.25 μM each of APDS and NPDS, while the non-equimolar reaction of intercalated disulfides (**PER2**, **PER3**) consisted of 100 μg/mL of APDS-TSM or Cyst-TSM with 0.5 μM of NPDS; this translates to roughly 60 μM or 50 μM of intercalated APDS or Cyst, respectively (based on calculated disulfide content from TGA results). These conditions push the reaction to consume NPDS. To assess the stability and reusability of the functionalized nanosheets, **PER2** was repeated using APDS-TSM that had been dispersed in DMSO and then redried (**PER2′**).

In the next series of experiments, **PER1-3** were repeated under the same conditions, but stopped after 20 min of UV radiation, then kept in a dark room at RT for 24 h before recording the UV-vis spectrum again. Additionally, the same mixture as **PER1** was left in a dark room at RT and the UV-vis spectrum was occasionally recorded to check if the exchange reaction proceeds in DMSO without catalysts or stimuli (so-called "indiscriminate").

Finally, in a cursory study on disulfide/thiol exchange, we used the same procedure as **PER2** but using β-ME (2 μM) in place of NPDS (**PER4**). Also, in connection with the acrylate film fabrication, two DMSO dispersions of APDS-TSM (200 μg/mL) and PETA (140 μM) were irradiated with either UV or visible light to confirm UV-induced radical generation.

Fabrication of TSM/acrylate films. Composite films of PETA and TSM were fabricated by photo-curing. Table S1 lists the composition of each film. Prior to fabrication, 80 mg of layered silicates (Na-TSM, APDS-TSM, or Cyst-TSM) were swollen in 2 mL of DMSO by gentle stirring for 2 h, then the paste was collected by centrifugation (3500 rpm, 5 min) and 0.06 g was mixed into 0.95 g of PETA in a centrifugal mixer (ARE-310, Thinky) at 2000 rpm for 5 min. Samples containing photoinitiator (TPO, 2 wt%) were mixed the same way, using 1.0 g of PETA. The mixtures appeared to have uniform

dispersion and no visible sedimentation occurred within 48 h of mixing. The freshly prepared mixtures were deposited on quartz slides with Kapton tape spacers and irradiated with UV via a xenon lamp (LAX-C100, Asahi Spectra; 3.4 mW/cm^2 @ 300 nm) at a distance of 50 mm. The acrylate polymerization was monitored by ATR-FTIR and the curing was stopped when the film became solid without tack. The resulting films (roughly 10×8×0.1 mm^3) were characterized by XRD, and the TSM content estimated by TGA.

An additional three films were fabricated by filtration technique, in order to confirm that S-S scission produces the thiyl radicals, not C-S scission. Na-TSM was intercalated with 4-aminophenyl sulfide (APS), which contains a thioether rather than disulfide linkage, by the same procedure as the disulfides to produce APS-TSM. Next, 0.1 g of intercalated silicate (APDS-TSM, Cyst-TSM, or APS-TSM) was dispersed in DMF (2 mL) with 0.1g of PETA by sonication for 2 min. The dispersions were transferred to quartz cuvettes and irradiated with UV (1.7 mW/cm^2 @ 300 nm) for 30 min, then vacuum-filtered and dried in a circulating oven at 40 °C for 72 h. The resulting films were then characterized by XRD.

Characterization. Disulfide reagents, intercalated silicate powders, and composite films were placed on glass holders and XRD patterns were recorded with an Ultima IV (Rigaku) using CuKα radiation (λ = 0.15406 nm) at 40 kV/30 mA and a scanning rate of 2°/min. UV-vis spectra in DMSO were recorded at concentrations over the range 0.25-10 μmol/L (reagents) or 20-200 μg/mL (silicates) using a UV-2450 spectrometer (Shimadzu) over the range 200-800 nm. Samples were placed on glass slides and Raman spectra were recorded at a resolution of 8.56 cm^{-1} on an NRS-7100 microspectrometer (JASCO) using laser wavelengths of 532 nm (reagents) or 785 nm (silicates), depending on the amount of fluorescence. The irradiation and accumulation time were 28.8 mW and 30 s, respectively. Silicate powder samples were placed on a diamond ATR crystal and spectra were recorded using an IR Affinity spectrometer (Shimadzu) over the range 400-4000 cm^{-1} at a resolution of 2 cm^{-1}. Acrylate film curing was monitored by the same ATR-FTIR over the range 400-2000 cm^{-1} at a resolution of 2 cm^{-1}. Baseline corrections and peak area calculations were performed according to the literature.[S2]

Thermal decomposition of the disulfide reagents and intercalated silicates was measured on a TG/DTA7300 (Hitachi Hi Tech) by heating approximately 2.5-3.0 mg of sample in a Pt pan from 20 to 1000 °C at a rate of 10 °C/min under N_2 atmosphere, and the amount of intercalated disulfide was calculated from the mass loss between roughly 150-650 °C. TSM powder samples were sprinkled onto conductive tape and sputter coated, then images were acquired on a Quanta 600 SEM (FEI) under high vacuum at 5 kV. Swelling and delamination was investigated by AFM: APDS-TSM powder was dispersed in water or DMSO (1 mg/mL) by bath sonication for 2 min, then mixed by a vertical rotating mixer for one day. A drop of the supernatant was deposited on a freshly cleaned sapphire wafer and the excess was removed by rinsing with acetone. Images were collected using tapping mode on an SFT-4500 (Shimadzu) equipped with a silicon probe (resonant frequency: 70 kHz; spring constant: 2 N/m).

Simulation Details. XRD patterns of APDS (depos. no. 928403) and Cyst (depos. no. 134759) were simulated from registered CIFs (CCFC) using Mercury.[S3] Raman spectra of APDS and Cyst were simulated using Gaussian16 at the B3LYP/6-31G**(d,p) level.[S4]

Acknowledgement

This work was financially supported by JSPS Kakenhi Grants No. 20K14617 and 22K05204. The authors thank M. Kamon and A. Iwanade (NIMS) for experimental support, and N.T. Hoang (RIKEN) for assistance with spectroscopic data processing.

References

1. Y. Zhao, W. Yang, Y. Xue, X. Wang and T. Lin, J. Mater. Chem., 2011, 21, 4869.
2. M. Nomi, M. Morita, A. Kondo and K. Maeda, Inorg. Chem., 2022, 61, 5255.
3. S. Ishihara, N. Iyi, Y. Tsujimoto, S. Tominaka, Y. Matsushita, V. Krishnan, M. Akada, J. Labuta, K. Deguchi, S. Ohki, M. Tansho, T. Shimizu, Q. Ji, Y. Yamauchi, J.P. Hill, H. Abe and K. Ariga, Chem. Commun., 2013, 49, 3631.
4. H. Hata, T.E. Mallouk and K. Kuroda, Chem. Mater., 2009, 21, 985.
5. S. Ma, Q. Chen, H. Li, P. Wang, S.M. Islam, Q. Gu, X. Yang and M.G. Kanatzidis, J. Mater. Chem. A, 2014, 2, 10280.
6. M.T. Gokmen, J. Brassinne, R.A. Prasath and F.E. Du Prez, Chem. Commun., 2011, 47, 4652.
7. O.F. Odio, L. Lartundo-Rojas, E.G. Palacios, R. Martinez and E. Reguera, Appl. Surf. Sci., 2016, 386, 160.
8. T. Eom and A. Khan, Chem. Commun., 2020, 56, 7419.
9. J. Li, L. Li, X. Du, W. Feng, A. Welle, L. Trapp, M. Grunze, M. Hirtz and P.A. Levkin, Nano Lett., 2015, 15, 675..
10. X. Du, J. Li, A. Welle, L. Li, W. Feng and P.A. Levkin, Adv. Mater., 2015, 27, 4997.
11. S. Nevejans, N. Ballard, J.I. Miranda, B. Reck and J.M. Asua, PCCP, 2016, 18, 27577.
12. F. Klepel and B.J. Ravoo, Org. Biomol. Chem., 2017, 15, 3840; J. Atcher and I. Alfonso, RSC Adv., 2013, 3, 25605.
13. U.F. Fritze and M. von Delius, Chem. Commun., 2016, 52, 6363.
14. D. Koyama and A.J. Orr-Ewing, PCCP, 2016, 18, 12115.
15. T. Bultmann and N.P. Ernsting, J. Phys. Chem., 1996, 100, 19416.
16. F. Vibert, S.R.A. Marque, E. Block, S. Queyroy, M.P. Bertrand, S. Gastaldi and E. Besson, Chem. Sci., 2014, 5, 4716.
17. Y. Ding, Y-P. Chen, X. Zhang, L. Chen, Z. Dong, H-L. Jiang, H. Xu and H-C. Zhou, J. Am. Chem. Soc., 2017, 139, 9136.
18. J. Wang, L. Fu, H. Yang, X. Zuo and D. Wu, J. Phys. Chem. Lett., 2021, 12, 9973.
19. J-G. Sun, W-Z. Weng, P. Li and B. Zhang, Green Chem., 2017, 19, 1128.
20. R. Koyilapu, S. Subhadarshini, S. Singha and T. Jana, Polymer, 2021, 212, 123175.
21. R. Koyilapu, S. Subhadarshini, S. Singha and T. Jana, Polymer, 2021, 212, 123175.
22. F. Djouani, F. Herbst, M.M. Chehimi and K. Benzarti, Surf. Interface Anal., 2010, 42, 1019.
23. S. Murugesan and T. Scheibel, Adv. Funct. Mater., 2020, 30, 1908101; P.N. Brevnov, A.S. Zabolotnov, V.G. Krasheninnikov, B.V. Pokid'ko, A.V. Bakirov, O.N. Babkina and L.A. Novokshonova, Kinet. Catal., 2016, 57, 482.
24.
25. N. P. Balsara, L. J. Fetters, N. Hadjichristidis, D. J. Lohse, C. C. Han, W. W. Graessley, R. Krishnamoorti, *Bull. Chem. Soc. Jpn.* **1999**, *32*, 6137.
26. …

Figure 1. Controllable photo-reactivity of disulfides through intercalation into layered materials. (a) Scheme of tethering strategy and the resulting photo-induced reactions. (b) XRD patterns and (c) illustration of intercalation structures of the functionalized silicates.

Figure 3. UV-vis spectra taken after 20 min of UV radiation and then again 24 h later, for (a) molecular APDS/NPDS (**PER1**), and (b) tethered APDS/NPDS (**PER2**). Disulfides participate in indiscriminate exchange reaction without UV radiation, but tethering them to nanosheets hinders the exchange reaction without UV light.

Graphical Abstract

<Title>

<Authors' names>

<Summary>
Length of summary should be about 50-60 words.

<Diagram>

A small diagram or other informative illustration that shows the most striking feature of the paper in pictorial form.

This size should be 4.8 × 4.8 cm or 10.0 × 3.0 cm.